

# Diffused vorticity approach to the oscillations of a rotating Bose-Einstein condensate confined in a harmonic plus quartic trap

M. Cozzini

*Dipartimento di Fisica, Università di Trento and BEC centre CNR-INFM,  
via Sommarive 14, I-38050 Povo (TN), Italy*

March 23, 2022

## Abstract

The collective modes of a rotating Bose-Einstein condensate confined in an attractive quadratic plus quartic trap are investigated. Assuming the presence of a large number of vortices we apply the diffused vorticity approach to the system. We then use the sum rule technique for the calculation of collective frequencies, comparing the results with the numerical solution of the linearized hydrodynamic equations. Numerical solutions also show the existence of low-frequency multipole modes which are interpreted as vortex oscillations.

## 1 Introduction

Quantized vortices are one of the most striking features of superfluids, ranging from liquid helium to superconductors. Bose-Einstein condensates of alkali gases have proved to be one of the best tools to study these fascinating quantum objects, presenting several advantages with respect to both helium and superconductors. On the other hand, due to the limited resolution imposed by current experimental techniques, direct in situ imaging of vortices is a very difficult task. This problem has been however overcome by using time-of-flight absorption images, which take advantage of the expansion of the gas after release of the trap.

In this context, particularly appealing structures are given by vortex arrays, where singly quantized vortices typically arrange in highly regular triangular lattices, similar to the Abrikosov lattice of superconductors. In order to realize such configurations, large amounts of angular momentum have to be transferred to the gas, what can be done by using various experimental procedures [1]. The acquired angular velocity tends then to enlarge the rotating cloud, the centrifugal force giving rise to bulge effects which flatten the density profile towards a 2D configuration. In the presence of purely harmonic confinement characterized by a frequency  $\omega_{\perp}$  in the plane of rotation, this phenomenon fixes an upper limit for the angular velocity  $\Omega$  of the system, namely the frequency  $\Omega = \omega_{\perp}$  at which the quadratic effective potential given by the centrifugal force exactly equals the harmonic trapping term. Beyond this angular velocity the centrifugal force dominates over the confinement and the system is no longer bounded.

The possibility of reaching arbitrarily high angular velocities is however provided by stronger than quadratic traps [2, 3, 4]. The introduction of a quartic term in the potential then opens up new regimes in the study of rotating condensates, making possible the realization of new equilibrium configurations with different vortex arrays.

In the present contribution, we will first briefly summarize the stationary solutions for an effectively two-dimensional Bose-Einstein condensate rotating in a harmonic plus quartic trap at zero temperature [5]. Then, within the Thomas-Fermi approximation [6], we will focus on the analysis of the most important collective excitations of the system [7]. Numerical solution of the hydrodynamic equations will be combined with the sum rule method. Vortex arrays will be treated within the so-called diffused vorticity approximation [8], thereby neglecting the microscopic motion of single vortices in favour of the macroscopic dynamics of the system. Nevertheless, signatures of vortex modes will also be found, although the corresponding predicted frequencies are not expected to be very accurate. Indeed, a consistent calculation of such effects would require a more detailed treatment, as the one of Ref. [9].

## 2 Stationary configurations

As anticipated above, in the presence of a large number of vortices, as always assumed in the following<sup>1</sup>, it is possible to use the so called diffused vorticity approach, consisting of averaging the velocity field  $\mathbf{v}$  over regions containing many vortex lines and assuming that the vorticity is spread continuously in the fluid. For example, in the case of a uniform vortex lattice with average vortex density  $n_v$ , this corresponds to assuming rigid body rotation  $\mathbf{v} = \mathbf{\Omega} \wedge \mathbf{r}$  with  $\mathbf{\Omega} = \hbar n_v / 2M$ , where  $M$  is the atomic mass. The relation between the effective angular velocity  $\mathbf{\Omega}$ , oriented along the vortex line direction, and the vortex density  $n_v$  can be derived by imposing that the circulation of the averaged velocity field around a single vortex cell be equal to  $\hbar/M$ , as for the single vortex case. More generally, the usual irrotationality condition  $\nabla \wedge \mathbf{v} = 0$  of superfluid hydrodynamics is broken in favour of  $\nabla \wedge \mathbf{v}(\mathbf{r}) = \hbar n_v(\mathbf{r})/M$ , where  $n_v(\mathbf{r})$  is the average vortex density in the proximity of point  $\mathbf{r}$ . It is then clear that the validity condition of this approach is that the average distance  $1/\sqrt{n_v}$  between vortices be much smaller than the size of the cloud<sup>2</sup>, the concept of diffused vorticity being adequate to describe the dynamics only at distances larger than  $1/\sqrt{n_v}$ . If in addition  $\xi \ll 1/\sqrt{n_v}$ , where  $\xi = \hbar/\sqrt{2gn}$  is the healing length defined in terms of the interaction coupling constant  $g$  and bulk density  $n$ , one can safely use the Thomas-Fermi approximation. Indeed, if the size of vortex cores fixed by  $\xi$  is much smaller than the inter-vortex distance, one can assume a slowly varying density profile between vortices, consequently neglecting density gradients associated with quantum pressure effects.

Within the presently discussed approximations, the system is then described by the rotational hydrodynamic equations, which in the rotating frame read

$$\frac{\partial n}{\partial t} + \nabla \cdot (n\mathbf{v}') = 0, \quad (1)$$

$$\frac{\partial \mathbf{v}'}{\partial t} + \nabla \cdot \left( \frac{v'^2}{2} + \frac{V_{\text{ext}}}{M} - \frac{|\mathbf{\Omega} \wedge \mathbf{r}|^2}{2} + \frac{gn}{M} \right) = \mathbf{v}' \wedge (\nabla \wedge \mathbf{v}') - 2\mathbf{\Omega} \wedge \mathbf{v}', \quad (2)$$

where  $n(\mathbf{r}, t)$  is the spatial density,  $\mathbf{v}'(\mathbf{r}, t) = \mathbf{v}(\mathbf{r}, t) - \mathbf{\Omega} \wedge \mathbf{r}$  is the velocity in the rotating frame, and  $V_{\text{ext}}$  is the external potential. It is trivial to check that  $\mathbf{v}_0 = \mathbf{\Omega} \wedge \mathbf{r}$ ,  $gn_0 = \mu - V_{\text{ext}} + M|\mathbf{\Omega} \wedge \mathbf{r}|^2/2$  is a stationary solution for the system, where  $\mu$ , fixed by the normalization condition  $\int n d\mathbf{r} = N$ , is the chemical potential in the rotating frame.

Although equilibrium configurations in Thomas-Fermi approximation can be obtained also for the 3D case [3], for simplicity we will consider only 2D configurations, which makes the analysis of collective excitations considerably easier. In fact, due to the repulsive

---

<sup>1</sup>For very large rotation rates the external potential considered here is predicted to give rise to giant vortex states [5], where all the vorticity is confined in a single hole. We do not discuss such configurations and always deal with the case where singly quantized vortices are present.

<sup>2</sup>For an annular structure one has to compare the average vortex distance with both the annulus radius and the annulus width.

centrifugal term  $-|\mathbf{\Omega} \wedge \mathbf{r}|^2/2$  in Eq. (2), which tends to flatten the equilibrium density  $n_0$ , this is a natural approximation for fast rotating condensates<sup>3</sup>. Instead of using the 3D coupling constant  $g_{3D} = 4\pi\hbar^2 a/M$ , where  $a$  is the usual 3D  $s$ -wave scattering length, we then introduce an effective 2D coupling constant  $g_{2D} = g_{3D}/Z$ , where  $Z$  is a proper length taking into account the extension of the real system along the rotation axis<sup>4</sup>.

The trapping potential is given by

$$V_{\text{ext}} = \frac{\hbar\omega_{\perp}}{2} \left( \frac{r^2}{d_{\perp}^2} + \lambda \frac{r^4}{d_{\perp}^4} \right), \quad (3)$$

where  $\omega_{\perp}$  is the harmonic oscillator frequency,  $d_{\perp} = \sqrt{\hbar/M\omega_{\perp}}$  is the characteristic harmonic oscillator length with the atomic mass  $M$ ,  $r = \sqrt{x^2 + y^2}$  is the two-dimensional radial coordinate, and  $\lambda$  is the dimensionless parameter characterizing the strength of the quartic term. In the following, we will use dimensionless harmonic oscillator units, where  $\omega_{\perp}$  and  $d_{\perp}$  are the units of frequency and length respectively.

The equation for  $n_0$  then becomes

$$n_0 = \frac{1}{g} \left[ \mu + \frac{\Omega^2 - 1}{2} r^2 - \frac{\lambda}{2} r^4 \right] = \frac{\lambda}{2g} (R_2^2 - r^2)(r^2 - R_1^2), \quad (4)$$

where  $g$  is the dimensionless coupling constant and

$$R_{1,2}^2 = \frac{\Omega^2 - 1}{2\lambda} \pm \sqrt{\left( \frac{\Omega^2 - 1}{2\lambda} \right)^2 + \frac{2\mu}{\lambda}}. \quad (5)$$

The density is assumed to be zero where the right hand side of Eq. (4) is negative. For  $\mu > 0$  the value of  $R_1$  becomes purely imaginary and the density vanishes at the radius  $R = R_2$ , while for  $\mu \leq 0$  two different radii  $R_{1,2}$  are present. This reflects the transition occurring at  $\mu = 0$ , where a hole forms in the centre of the condensate and the density profile assumes an annular shape. From the normalization condition one can calculate the transition angular velocity  $\Omega_h$  obtaining  $\Omega_h^2 = 1 + (12\lambda^2 g N / \pi)^{1/3}$  [5].

For the case  $\Omega < \Omega_h$ , when the hole is absent, expressing  $R_1$  in terms of  $R_2 = R$  as  $R_1^2 = (\Omega^2 - 1)/\lambda - R^2$ , the normalization condition gives the following third degree equation for  $R^2$

$$R^4(4\lambda R^2 - 3\Omega^2 + 3) = \frac{12gN}{\pi}, \quad (6)$$

while the chemical potential becomes  $\mu = R^2(\lambda R^2 - \Omega^2 + 1)/2$ . In the following we will also need the expectation values  $\langle r^2 \rangle = \int n_0 r^2 d\mathbf{r}/N = \pi R^6(3\lambda R^2 - 2\Omega^2 + 2)/24gN$  and  $\langle r^4 \rangle = \pi R^8(8\lambda R^2 - 5\Omega^2 + 5)/120gN$ .

For the case  $\Omega > \Omega_h$ , defining  $R_{\pm}^2 = R_2^2 \pm R_1^2$  the normalization condition simply gives

$$\lambda R_{\pm}^6 = \frac{12gN}{\pi}, \quad (7)$$

and hence  $R_+^2 = (\Omega^2 - 1)/\lambda$  and  $R_-^2 = (\Omega_h^2 - 1)/\lambda$ . The chemical potential is now  $\mu = -\lambda(R_+^4 - R_-^4)/8$  and the previously defined expectation values become  $\langle r^2 \rangle = R_+^2/2$  and  $\langle r^4 \rangle = (5R_+^4 + R_-^4)/20$ .

---

<sup>3</sup>For small angular velocities one needs the additional assumption that a strong confinement in the axial direction is present.

<sup>4</sup>For a system uniform along the  $z$ -direction  $Z$  corresponds to the vertical size, while in the case of strong axial harmonic confinement one has  $Z = \sqrt{2\pi}a_z$ , where  $a_z$  is the oscillator length in the same direction.

### 3 Collective modes

The collective oscillations of the system in the Thomas-Fermi approximation can be found by linearizing the hydrodynamic equations (1) and (2), which become

$$\frac{\partial}{\partial t} \delta n + \nabla \cdot (n_0 \delta \mathbf{v}) = 0, \quad (8)$$

$$\frac{\partial}{\partial t} \delta \mathbf{v} + g \nabla \delta n + 2 \Omega \wedge \delta \mathbf{v} = 0. \quad (9)$$

These equations can be solved by expressing the radial and azimuthal components  $\delta v_r$  and  $\delta v_\phi$  of the velocity field in terms of  $\delta n$  and looking for solutions of the form  $\delta n = \delta n(r) e^{im\phi} e^{-i\omega t}$ , where  $m$  is the azimuthal quantum number,  $\phi$  is the azimuthal angle and  $\omega$  is the excitation frequency in the rotating frame. This gives<sup>5</sup>

$$(\omega^2 - 4\Omega^2) \delta v_r = i \left( -\omega \partial_r + \frac{2m\Omega}{r} \right) g \delta n, \quad (10)$$

$$(\omega^2 - 4\Omega^2) \delta v_\phi = \left( -2\Omega \partial_r + \frac{m\omega}{r} \right) g \delta n, \quad (11)$$

$$\omega \left[ \omega^2 - 4\Omega^2 - \frac{m^2 g n_0}{r^2} \right] \delta n - \frac{2m\Omega}{r} \frac{\partial(g n_0)}{\partial r} \delta n + \frac{\omega}{r} \frac{\partial}{\partial r} \left( r g n_0 \frac{\partial \delta n}{\partial r} \right) = 0. \quad (12)$$

At first sight, one could expect that the last equation depends both on  $gN$  and  $\lambda$ . Actually, only a given combination of these parameters really matters: in particular, for given  $\Omega$  and  $m$ , the solution is uniquely fixed by the value of  $\Omega_h$ , i.e. by the product  $\lambda^2 g N$ .

Eq. (12) can be significantly simplified in the large  $\Omega$  limit [7], where useful analytical results can be obtained. In general, however, this equation has to be solved numerically, what can be achieved by direct integration with the natural initial condition<sup>6</sup>

$$\frac{\partial \delta n}{\partial r}(R_2) = \frac{\omega(\omega^2 - 4\Omega^2) + 2m\Omega\lambda(R_2^2 - R_1^2)}{\omega\lambda R_2(R_2^2 - R_1^2)} \delta n(R_2) \quad (13)$$

and by varying  $\omega$  in order to obtain a well behaved solution. This procedure can be easily automatized by checking the validity of a condition similar to Eq. (13) for the final integration point  $r = 0$  for  $\Omega < \Omega_h$  and  $r = R_1$  for  $\Omega > \Omega_h$  and essentially corresponds to the so called shooting method described in Ref. [10]. The code has also been checked [11] against the relaxation method [10].

To obtain analytical results also below the large  $\Omega$  limit, we will rely on the sum rule method. To this purpose we introduce the  $p$ -energy weighted moments

$$m_p(F) = \sum_n \sigma_n(F) E_{n0}^p \quad (14)$$

relative to a generic excitation operator  $F = \sum_{k=1}^N f(\mathbf{r}_k)$ , where  $E_{n0}$  is the energy difference between the excited state  $|n\rangle$  and the ground state  $|0\rangle$ , and  $\sigma_n(F) = |\langle n|F|0\rangle|^2$  is the associated strength. We also define

$$m_p^\pm(F) = m_p(F) \pm m_p(F^\dagger). \quad (15)$$

Notice that for hermitian operators  $F = F^\dagger$  one simply has  $m_p^+(F) = 2m_p(F)$  and  $m_p^-(F) = 0$ .

---

<sup>5</sup>It is worth noticing that not all the solutions of Eq. (12) correspond to physical density variations. Indeed, in general one has to check that the resulting eigenfunctions preserve the density normalization  $\int \delta n d\mathbf{r} = 0$  and that the corresponding velocity variations are finite. The latter condition, for example, leads to the exclusion of the solutions with  $\omega = 2\Omega$ .

<sup>6</sup>In fact, density boundaries are regular singular points of Eq. (12). For these points the second derivative term cancels. Notice also that one can arbitrarily fix the value of  $\delta n(R_2)$ , this choice being equivalent to imposing the amplitude of the oscillation.

The energy weighted moments can be used to derive rigorous upper bounds for the excitation frequencies of the system [12]. For example, one has the following inequality for the lowest energy  $\hbar\omega_{\min}$  excited by the operator  $F$

$$(\hbar\omega_{\min})^s \leq \frac{m_{p+s}^+(F)}{m_p^+(F)}, \quad (16)$$

where  $s$  is positive and the equality holds whenever  $F$  excites one single mode. The explicit calculation of the moments  $m_{2p+1}^+(F)$  and  $m_{2p}^-(F)$  for  $p \geq 0$  can be carried out in terms of commutators between the excitation operator and the total Hamiltonian of the system, evaluated on the ground state. In addition, one has the important result  $m_{-1}^+(F) = -\chi_F(0)$ , which relates the useful inverse energy weighted moment to the static limit of the dynamic response function  $\chi_F(\omega)$ .

We first consider the lowest axisymmetric ( $m = 0$ ) mode. One expects that this breathing oscillation is mainly excited by the monopole operator  $\mathcal{M} = \sum_{k=1}^N r_k^2$ , although such perturbation, due to the presence of the quartic term in the potential, slightly couples also to higher modes<sup>7</sup>. Then, as usual, we extract the frequency of the lowest excited mode from the ratio between the energy weighted ( $m_1$ ) and inverse energy weighted ( $m_{-1}$ ) moments. Indeed, as evident from Eq. (14), low order moments minimize the contributions coming from higher eigenfrequencies<sup>8</sup>. The  $m_1$  moment for a hermitian operator can be expressed in terms of commutators as  $m_1(F) = \langle 0|[F, [H, F]]|0\rangle/2$ . Here the many-body Hamiltonian  $H$  in the rotating frame, with an obvious meaning of the symbols, is given by  $H = H_{\text{kin}} + H_{\text{ext}} + H_{\text{int}} - \Omega L_z$ , where the interaction term is  $H_{\text{int}} = g \sum_{i < j} \delta(\mathbf{r}_i - \mathbf{r}_j)$ . For the monopole operator one has  $[\mathcal{M}, [H, \mathcal{M}]] = 2\mathcal{M}$  and hence  $m_1(\mathcal{M}) = 2N\langle r^2 \rangle$ . On the other hand, since adding a static monopole perturbation to the Hamiltonian is equivalent to renormalizing the trapping frequency [12], the monopole static response can be calculated from  $\delta\langle r^2 \rangle = \chi_{\mathcal{M}}(0)M\delta\omega_{\perp}^2/2N = (\partial\langle r^2 \rangle/\partial\omega_{\perp}^2)\delta\omega_{\perp}^2$  (in dimensional units), where the derivative has to be calculated at constant angular momentum. Then, recalling that  $m_{-1}(\mathcal{M}) = -\chi_{\mathcal{M}}(0)/2$ , in the Thomas-Fermi approximation one finds

$$\omega^2 = \frac{m_1(\mathcal{M})}{m_{-1}(\mathcal{M})} = \begin{cases} 6\lambda R^2 + 4 & (\Omega < \Omega_h) \\ 6\lambda R_+^2 + 4 & (\Omega > \Omega_h) \end{cases}, \quad (17)$$

where the two expressions coincide for  $\Omega = \Omega_h$ . For  $\Omega > \Omega_h$ , since  $R_+^2 = (R_1^2 + R_2^2) = (\Omega^2 - 1)/\lambda$ , one finds the simple result  $\omega = \sqrt{6\Omega^2 - 2}$ .

Sum rule and hydrodynamic results are reported in Fig. 1. The agreement between the sum rule estimate and the numerical solution of Eq. (12) is quite good, confirming the hypothesis that the chosen moments are essentially saturated by the lowest  $m = 0$  mode. It is worth noticing that close to the critical angular velocity  $\Omega_h$  the Thomas-Fermi approximation is expected to fail, because quantum pressure effects become important in the inner region of vanishing density. The sharp transition shown in the sum rule result and the corresponding dimple in the hydrodynamic data are in fact smoothed out by the full Gross-Pitaevskii solution [7].

We now switch to excitations of the form  $f(\mathbf{r}) = r^{|m|}e^{im\phi}$ , which carry multiplicities different from zero. In particular we will concentrate on the quadrupole ( $m = 2$ ) operator  $\mathcal{Q}$ . The situation turns out to be much more complicated than for the monopole operator and one has to include in the analysis a larger number of moments, treating separately the two regions below and above  $\Omega_h$ .

Concerning the case  $\Omega < \Omega_h$ , one can proceed exactly as in the case of purely harmonic trapping [13] making a simple 2-mode assumption and solving the corresponding algebraic system given by the  $m_{-1}^+$ ,  $m_0^-$ ,  $m_1^+$ , and  $m_2^-$  moments. Indeed one expects that the low

<sup>7</sup>In the case of purely harmonic trapping the monopole operator is instead the exact one.

<sup>8</sup>On the other side, the coupling of the monopole operator with the next  $m = 0$  mode can be put in evidence by taking the  $m_3/m_1$  ratio, which is significantly higher than the chosen one.

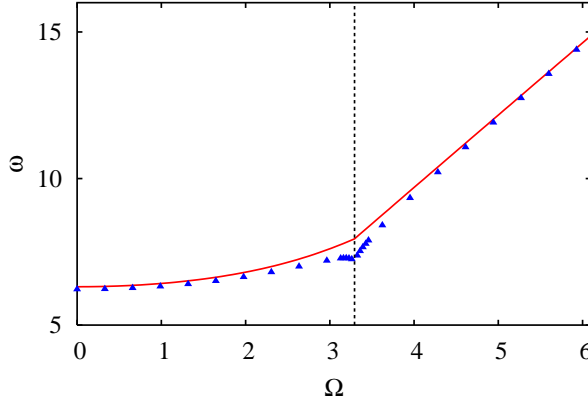


Figure 1: Lowest  $m = 0$  mode frequency as a function of the angular velocity for  $\lambda = 0.5$ ,  $gN = 1000$  (frequencies are in harmonic oscillator units). The solid line is the sum rule estimate, while the triangles are obtained from the numerical solution of Eq. (12). The dashed vertical line marks the critical angular velocity  $\Omega_h = 3.2935$ .

order moments of the quadrupole operator are saturated by the two lowest modes, the coupling with higher modes being negligible. Since  $m_0^-(\mathcal{Q}) = \langle 0 | [\mathcal{Q}^\dagger, \mathcal{Q}] | 0 \rangle = 0$ , the 2-mode assumption implies that the strengths of the considered  $m = \pm 2$  modes are equal. A simple calculation then shows that the resulting frequencies are

$$\omega(m = \pm 2) = \frac{1}{2} \left[ \sqrt{\left( \frac{m_2^-}{m_1^+} \right)^2 + 4 \frac{m_1^+}{m_{-1}^+}} \pm \frac{m_2^-}{m_1^+} \right], \quad (18)$$

while for the strengths we have  $\sigma_{m=+2}(\mathcal{Q}) = \sigma_{m=-2}(\mathcal{Q}^\dagger) = m_1^+ / [\omega(m = +2) + \omega(m = -2)]$ . For the explicit calculation of the  $m_1^+$  and  $m_2^-$  moments in the rotating frame sum rules give

$$m_1^+(\mathcal{Q}) = \langle 0 | [\mathcal{Q}^\dagger, [H, \mathcal{Q}]] | 0 \rangle = 8N \langle r^2 \rangle, \quad (19)$$

$$m_2^-(\mathcal{Q}) = \langle 0 | [[\mathcal{Q}^\dagger, H], [H, \mathcal{Q}]] | 0 \rangle = -16N(2\Omega \langle r^2 \rangle - \langle \ell_z \rangle), \quad (20)$$

where  $\ell_z = -i\partial/\partial\phi$ . Since in the Thomas-Fermi diffused vorticity approach the equilibrium velocity is  $\mathbf{v}_0 = \boldsymbol{\Omega} \wedge \mathbf{r}$ , so that  $\langle \ell_z \rangle = \Omega \langle r^2 \rangle$ , one simply finds  $m_2^-/m_1^+ = -2\Omega$ . In the same approximation, from the static quadrupole response one has instead  $m_{-1}^+ = \pi R^6/3g$  and hence  $m_1^+/m_{-1}^+ = 3\lambda R^2 - 2\Omega^2 + 2$ . Finally

$$\omega(m = \pm 2) = \sqrt{3\lambda R^2 - \Omega^2 + 2} \mp \Omega. \quad (21)$$

At  $\Omega = 0$  the two lowest  $m = \pm 2$  modes are degenerate, but, as soon as some vorticity enters the system, a splitting between the modes arises<sup>9</sup>. In the rotating frame, one can then distinguish between a low-lying and a high-lying branch, with azimuthal quantum number  $m = +2$  and  $m = -2$  respectively.

When  $\Omega > \Omega_h$ , both the low and high-lying branch acquire an additional mode, as shown by the hydrodynamic numerical results reported in Fig. 2. These new modes, which have opposite azimuthal quantum numbers with respect to the old ones, do not have

<sup>9</sup>Notice that at low angular velocities, when only a small number of vortices is present, the validity conditions of the diffused vorticity approach are not satisfied, so that Eq. (21) is only a rough approximation. At  $\Omega = 0$ , however, it gives the correct Thomas-Fermi result.

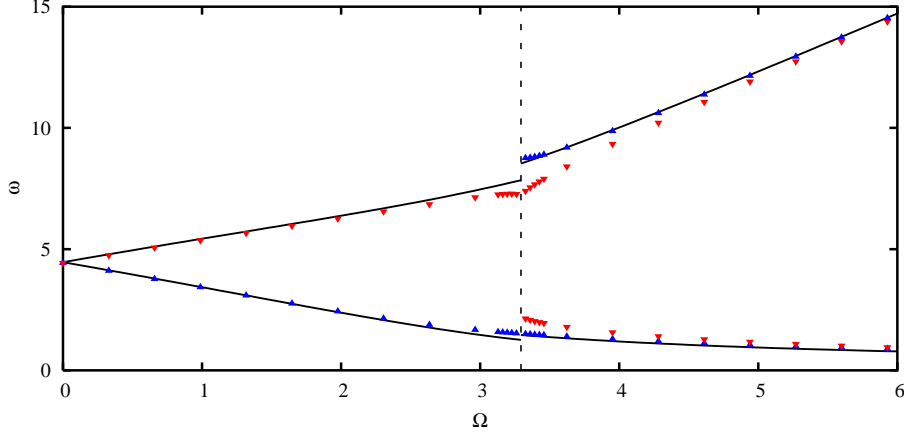


Figure 2: Excitation frequency as a function of the angular velocity for the main  $m = +2$  (upward triangles) and  $m = -2$  (downward triangles) modes for the same parameters as in Fig. 1. The dashed vertical line corresponds to  $\Omega = \Omega_h$ , while the solid lines correspond to the sum rule predictions discussed in the text.

any counterpart for  $\Omega < \Omega_h$  and arise due to the annular structure of the condensate. Their frequencies turn out to be very close to those of their previously discussed partners, becoming exactly degenerate in the large  $\Omega$  limit [7]. Hence, since a full treatment of the 4-mode system would be very complicated, we base our sum rule analysis on the assumption that two doubly degenerate energy levels are present. In order to calculate the resulting six unknown quantities  $\omega_{H,L}$ ,  $\sigma_{H,L}(\mathcal{Q})$ , and  $\sigma_{H,L}(\mathcal{Q}^\dagger)$ , one needs two more moments, namely

$$\begin{aligned} m_3^+(\mathcal{Q}) &= \langle 0 | [[[\mathcal{Q}^\dagger, H], [H, [H, \mathcal{Q}]]] | 0 \rangle = \\ &= 16N[(6\Omega^2 + 1)\langle r^2 \rangle + \langle p^2 \rangle + 3\lambda\langle r^4 \rangle - 6\Omega\langle \ell_z \rangle] , \end{aligned} \quad (22)$$

$$\begin{aligned} m_4^-(\mathcal{Q}) &= \langle 0 | [[[[\mathcal{Q}^\dagger, H], H], [H, [H, \mathcal{Q}]]] | 0 \rangle = \\ &= -64N[2\Omega(2\Omega^2 + 1)\langle r^2 \rangle + 2\Omega\langle p^2 \rangle - (6\Omega^2 + 1)\langle \ell_z \rangle + \\ &\quad + 3\lambda(2\Omega\langle r^4 \rangle - \langle r^2 \ell_z \rangle)] , \end{aligned} \quad (23)$$

where  $p^2 = -(\partial^2/\partial x^2 + \partial^2/\partial y^2)$ . The solution of the corresponding algebraic system gives

$$\omega_{H,L}^2 = \frac{1}{2} \left[ \frac{m_4^-}{m_2^-} \pm \sqrt{\left( \frac{m_4^-}{m_2^-} \right)^2 - 4 \frac{m_1^+}{m_{-1}^+} \left( \frac{m_4^-}{m_2^-} - \frac{m_3^+}{m_1^+} \right)} \right] , \quad (24)$$

$$\sigma_{H,L}(\mathcal{Q}) = \pm \frac{1}{2} \frac{(m_1^+ - m_{-1}^+ \omega_{L,H}^2) \omega_{H,L} + m_2^-}{\omega_H^2 - \omega_L^2} , \quad (25)$$

$$\sigma_{H,L}(\mathcal{Q}^\dagger) = \pm \frac{1}{2} \frac{(m_1^+ - m_{-1}^+ \omega_{L,H}^2) \omega_{H,L} - m_2^-}{\omega_H^2 - \omega_L^2} , \quad (26)$$

where, by using the Thomas-Fermi results  $\langle \ell_z \rangle = \Omega \langle r^2 \rangle$ ,  $\langle p^2 \rangle = \Omega^2 \langle r^2 \rangle$  and  $m_{-1}^+ = \pi(R_2^6 - R_1^6)/3g$ , one has  $m_1^+/m_{-1}^+ = 4(\Omega^2 - 1)\lambda^2 R_-^4/[3(\Omega^2 - 1)^2 + \lambda^2 R_-^4]$ ,  $m_3^+/m_1^+ = 5\Omega^2 - 1 + (3/5)\lambda^2 R_-^4/(\Omega^2 - 1)$  and  $m_4^-/m_2^- = 6\Omega^2 - 2 + (6/5)\lambda^2 R_-^4/(\Omega^2 - 1)$ . Recalling that  $\lambda R_-^2 = \Omega_h^2 - 1$ , one can then rewrite the frequencies as

$$\begin{aligned} \omega_{H,L}^2 &= 3\Omega^2 - 1 + \frac{3}{5} \frac{(\Omega_h^2 - 1)^2}{\Omega^2 - 1} + \\ &\pm \sqrt{\left( 3\Omega^2 - 1 + \frac{3}{5} \frac{(\Omega_h^2 - 1)^2}{\Omega^2 - 1} \right)^2 - \frac{4}{5} \frac{5(\Omega^2 - 1)^2 + 3(\Omega_h^2 - 1)^2}{3(\Omega^2 - 1)^2 + (\Omega_h^2 - 1)^2}} . \end{aligned} \quad (27)$$

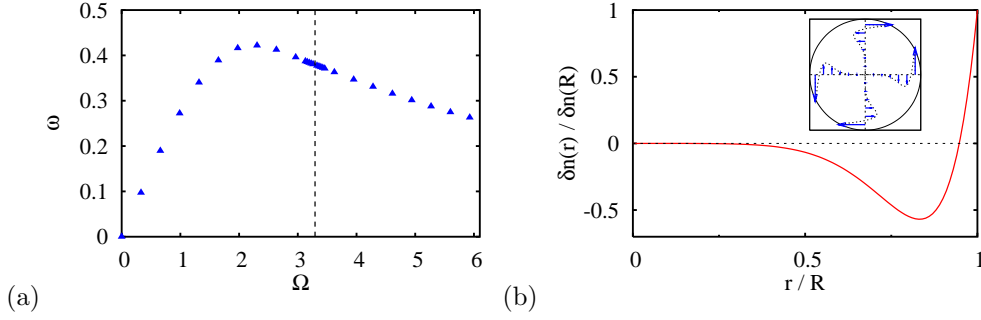


Figure 3: Behaviour of the  $m = +2$  vortex mode with the lowest number of radial nodes for the same parameters as in Fig. 1: (a) excitation frequency  $\omega$  as a function of the angular velocity  $\Omega$  (the dashed vertical line corresponds to  $\Omega = \Omega_h$ ); (b) radial dependence of the density variation at  $\Omega = 0.9 \Omega_h$  ( $\omega = 0.396$ ), the angular dependence being simply given by  $e^{i2\phi}$ . In the inset, the azimuthal component  $\delta v_\phi$  of the velocity variation is shown for the angles  $\phi = 0, \pi/2, \pi, 3\pi/2$ .

The results predicted by Eqs. (21) and (27) are reported in Fig. 2. An analysis of the strengths given by Eqs. (25) and (26) shows that at  $\Omega = \Omega_h$  only the old modes are significantly excited. However, with increasing  $\Omega$ , while the  $m = +2$  high-lying mode still has vanishing strength, the  $m = -2$  low-lying mode becomes more and more important, eventually even overcoming the contribution given by the high-lying  $m = -2$  mode [7]. It is also worth noticing that in the large  $\Omega$  limit the high-lying frequency is essentially given by  $\sqrt{m_4^-/m_2^-}$  and one has  $\omega_H^2 = 6\Omega^2 - 2$  as for the monopole mode. In the same limit, the low-lying frequency is given by  $\omega_L = (\sqrt{2}/3)(\Omega_h^2 - 1)/\Omega$  [7]. If one had used the same 2-mode assumption discussed for  $\Omega < \Omega_h$  also for  $\Omega > \Omega_h$ , the resulting values would have largely underestimated the correct frequencies. Finally, we notice that the same procedure could be used to extract the dipole frequencies.

In the last part of this section we are going to discuss another class of modes found from the numerical solution of the hydrodynamic equations. Indeed, numerical calculations show the presence of very low frequency multipole modes which cannot be interpreted in terms of sound propagation. One can still label these excitations with the azimuthal quantum number  $m$  and the number of radial nodes. The frequencies of the  $m = +2$  modes with the lowest number of radial nodes are plotted in Fig. 3(a) as a function of the angular velocity. It emerges that these modes are present on both sides of the critical angular velocity  $\Omega_h$  and that their frequency is zero for  $\Omega = 0$ . The rotational origin of these excitations together with their very low frequencies induces to identify these oscillations as multipole vortex modes, belonging to the family of Tkachenko modes already studied in harmonically trapped condensates [14, 15, 16, 17]. In order to further investigate this hypothesis one can calculate the corresponding velocity variation, which indeed, at least for  $\Omega < \Omega_h$  where the central hole is absent, resembles the typical lattice distortions of Tkachenko modes. This is shown in the inset of Fig. 3(b), where the azimuthal component  $\delta v_\phi$  of the velocity variation is plotted, the radial component  $\delta v_r$  being practically negligible.

Concerning the multipolarity of the modes, a simple remark is in order here. As noted in Ref. [18], rotational hydrodynamic equations admit a class of zero energy solutions which may be interpreted as Tkachenko modes. More in detail, any zero frequency solution of Eqs. (8) and (9) obeys the relation

$$\delta \mathbf{v} = \frac{2\Omega}{\Omega^2} \wedge \nabla g \delta n, \quad (28)$$

which implies  $\nabla \cdot \delta \mathbf{v} = 0$ . Hence, substituting into Eq. (8) and using  $\partial n_0 / \partial \phi = 0$ , valid for



an axisymmetric equilibrium density profile, one finds

$$\frac{\partial}{\partial \phi} \delta n = 0, \quad (29)$$

so that these modes must correspond to  $m = 0$ . It follows that all the  $m \neq 0$  modes, included Tkachenko ones, cannot have zero frequency in the diffused vorticity approach. However, due to the crude approximation used to treat vorticity within this method, one does not expect the predicted frequencies to be very accurate.

Actually, it turns out that the numerical frequencies *decrease* by increasing the number of radial nodes. This is probably related to the fact that the nodes accumulate in the proximity of the cloud boundary, where the Thomas-Fermi approximation is expected to fail. This situation is similar to the case of the  $m = 0$  breathing mode at the critical angular velocity  $\Omega_h$ , where the frequencies plotted in Fig. 1 show an unphysical dimple not present in the full Gross-Pitaevskii simulations. It is also worth noticing that the absence of such dimple in the positive  $m$  modes of Figs. 2 and 3(a) is indeed due to the fact that these oscillations are concentrated on the external boundary (see Fig. 3(b)), so that the quality of the approximation used to treat the central density at  $\Omega = \Omega_h$  does not affect their frequency.

According to the proposed picture, the same class of solutions of the rotational hydrodynamic equations must be present also for a purely harmonic potential. This is indeed the case. For the  $m = +2$  mode with the lowest number of radial nodes, where the predicted frequency is expected to be more reliable, in the frame rotating at  $\Omega = 0.7$  one finds  $\omega = 0.204$  (in units of the harmonic trapping frequency). Note that for 2D harmonic trapping the usual multipole modes in the rotating frame can be found analytically according to the formula  $\omega(\pm|m|) = \sqrt{2|m| - (|m| - 1)\Omega^2} \mp \Omega$ , identical to the 3D result found in Ref. [18]. For the harmonic case, in addition, once the radial distance is expressed in units of the Thomas-Fermi radius<sup>10</sup>, Eq. (12) depends only on  $m$  and  $\Omega$ , so that all the eigenfrequencies are independent of the interaction. The diffused vorticity estimate of the multipole Tkachenko frequencies, consequently, cannot properly include the compressibility effects which have already proven to be important for the  $m = 0$  case [16]. Nevertheless, the comparison with the calculations available in the literature [19] shows that the order of magnitude of the predicted frequencies is correct.

## 4 Conclusions

In this paper we have presented the numerical solution of the two-dimensional linearized rotational hydrodynamic equations and an accurate sum rule analysis for the monopole and quadrupole modes of a rotating condensate in a harmonic plus quartic trap, offering a discussion complementary to the work contained in Ref. [7]. The numerical results for the monopole and high-lying quadrupole modes have revealed shortcomings in using the Thomas-Fermi approximation rather than the full Gross-Pitaevskii solution [7] near to the critical angular frequency  $\Omega_h$  for hole formation. The frequency  $\Omega_h$  has also been identified as the threshold angular frequency where additional modes appear, due to the new geometry of the system. On the other hand, sum rules have provided reliable analytical estimates for the frequencies and for the excitation strengths of the considered modes. Finally, it has been shown that the multipole vortex oscillations have a non-zero energy counterpart in the diffused vorticity approach, in contrast to the  $m = 0$  Tkachenko modes. The corresponding frequency estimate is however expected to be scarcely precise, due to the same effects which lower to zero the energy in the  $m = 0$  case.

I warmly thank B. Jackson, A.L. Fetter, and S. Stringari for their precious suggestions.

---

<sup>10</sup>In physical units, the Thomas-Fermi equilibrium density for the 2D harmonic oscillator is  $gn_0 = (M/2)(\omega_\perp^2 - \Omega^2)R^2(1 - r^2/R^2)$ .

## References

- [1] K.W. Madison, F. Chevy, W. Wohlleben, and J. Dalibard, J. Mod. Opt. **47**, 2715 (2000); J.R. Abo-Shaeer, C. Raman, J.M. Vogels, W. Ketterle, Science **292**, 476 (2001); P.C. Haljan, I. Coddington, P. Engels, and E.A. Cornell, Phys. Rev. Lett. **87**, 210403 (2001).
- [2] V. Bretin, S. Stock, Y. Seurin, and J. Dalibard, Phys. Rev. Lett. **92**, 050403 (2004); S. Stock, V. Bretin, F. Chevy, and J. Dalibard, Europhys. Lett. **65**, 594 (2004).
- [3] A.L. Fetter, Phys. Rev. A **64**, 063608 (2001); A. Aftalion and I. Danaila, Phys. Rev. A **69**, 033608 (2004); I. Danaila, Phys. Rev. A **72**, 013605 (2005).
- [4] U.R. Fischer and G. Baym, Phys. Rev. Lett. **90**, 140402 (2003); G.M. Kavoulakis and G. Baym, New J. Phys. **5**, 51 (2003); E. Lundh, Phys. Rev. A **65**, 043604 (2002); A.D. Jackson, G.M. Kavoulakis, and E. Lundh, Phys. Rev. A **69**, 053619 (2004); A.D. Jackson and G.M. Kavoulakis, Phys. Rev. A **70**, 023601 (2004).
- [5] A.L. Fetter, B. Jackson, and S. Stringari, Phys. Rev. A **71**, 013605 (2005).
- [6] F. Dalfovo, S. Giorgini, L. Pitaevskii, and S. Stringari, Rev. Mod. Phys. **71**, 463 (1999).
- [7] M. Cozzini, A.L. Fetter, B. Jackson, and S. Stringari, Phys. Rev. Lett. **94**, 100402 (2005).
- [8] M. Cozzini and S. Stringari, Phys. Rev. A **67**, 041602(R) (2003).
- [9] G. Baym and E. Chandler, J. Low Temp. Phys. **50**, 57 (1983).
- [10] W.H. Press, S.A. Teukolsky, W.T. Vetterling, B.P. Flannery, *Numerical Recipes in FORTRAN, 2nd Edition* (Cambridge University Press, Cambridge, 1992).
- [11] B. Jackson, private communication.
- [12] L. P. Pitaevskii and S. Stringari, *Bose-Einstein Condensation* (Oxford University Press, Oxford, 2003).
- [13] F. Zambelli and S. Stringari, Phys. Rev. Lett. **81**, 1754 (1998).
- [14] I. Coddington, P. Engels, V. Schweikhard, and E.A. Cornell, Phys. Rev. Lett. **91**, 100402 (2003).
- [15] G. Baym, Phys. Rev. Lett. **91**, 110402 (2003).
- [16] M. Cozzini, L.P. Pitaevskii, and S. Stringari, Phys. Rev. Lett. **92**, 220401 (2004).
- [17] E.B. Sonin, Phys. Rev. A **71**, 011603 (2005).
- [18] F. Chevy and S. Stringari, Phys. Rev. A **68**, 053601 (2003).
- [19] T. Mizushima *et al.*, Phys. Rev. Lett. **92**, 060407 (2004).